

TWELFTH EUROPEAN ROTORCRAFT FORUM

Paper No. 21

A UNIFIED APPROACH FOR POTENTIAL AND VISCOUS
FREE-WAKE ANALYSIS OF HELICOPTER ROTORS

L. Morino and B. K. Bharadvaj

Boston University

Boston, USA

September 22 - 25, 1986

Garmisch-Partenkirchen
Federal Republic of Germany

Deutsche Gesellschaft für Luft- und Raumfahrt e. V. (DGLR)
Godesberger Allee 70, D-5300 Bonn 2, F.R.G.

A UNIFIED APPROACH FOR POTENTIAL AND VISCOUS FREE-WAKE ANALYSIS OF HELICOPTER ROTORS

L. Morino and B. K. Bharadvaj
Boston University, Boston, USA

Abstract

A unified formulation for the potential and viscous free-wake analysis of helicopter rotors in incompressible, flows is presented. The wake is treated as a vortex layer (with zero thickness for potential flows and finite thickness for viscous flows). The numerical algorithm for the discretization is outlined. Numerical results are in good agreement with the numerical results of Rao and Schatzle and the experimental ones of Landgrebe and of Shivananda.

1. Introduction.

Accurate computations of loads on rotor blades are required in many aspects of helicopter design, such as performance, structural analysis and aeroelasticity. In all these cases, the wake geometry is an essential aspect of the problem. Two approaches are commonly used to address the issue. In the first, the wake is prescribed, typically using an analytical expression that is obtained from the interpolation of experimental results (generalized-wake analysis). In the second, the wake geometry is treated as one of the unknowns of the problem (free-wake analysis). This paper deals with the second approach. Past work on free-wake analysis (see, e.g., Refs. 1-10) is limited to potential flows. The wake may be described either as a doublet layer or as a vortex layer. A review of the two approaches is given by Sipic and Morino⁹, and Kandil¹⁰, respectively.

It is the general consensus that the free-wake analysis of viscous flows is a formidable task, considerably more complex than potential-flow analysis. It is the objective of this paper to demonstrate that the viscous-flow analysis may be almost as simple as the potential-flow analysis, at least for attached flows. This paper is based on the work of Morino and Bharadvaj¹¹ where a general methodology for the free-wake analysis of helicopter rotors for incompressible flows (potential and viscous), was presented. Reference 11 is a comprehensive report, which includes the theoretical formulation, the numerical algorithm, and application to the free-wake analysis of helicopter rotors. The more theoretical aspects of Ref. 11, in particular the relationship of the formulation with the Helmholtz decomposition, were presented by Morino, Bharadvaj and Del Marco¹². The computational aspects of Ref. 11, in particular the relationship of the methodology to the boundary-element method were presented by Bharadvaj and Morino¹³.

The present paper emphasizes the application of the methodology to the problem of free-wake analysis of helicopter rotors and is aimed at the helicopter aerodynamics community. The theoretical derivations are reduced to a minimum and the formulation is presented as a natural extension of that for potential flows (thereby avoiding the use of the Helmholtz decomposition, which is necessary in order to give a rigorous derivation of the viscous-flow formulation). This has the advantage of simplifying the derivation of the formulation as well as showing the simplicity of the resulting algorithm (which involves only a minor additional calculation over the potential flow algorithm). A more rigorous derivation of the formulation is presented in Ref. 12. A comprehensive analysis of the issue of the boundary conditions for the Helmholtz decomposition is presented by Morino¹⁴.

2. Potential Doublet-Wake Formulation

In order to introduce the formulation used here, for both potential and viscous flows, it is convenient to start from the potential-flow formulation introduced by Morino et al.⁸, which is briefly summarized here. If the flow field of an inviscid incompressible fluid is

initially irrotational, it remains irrotational at all times except for the points of the wake, and therefore, except for those points, the velocity may be expressed as

$$\mathbf{v} = \nabla\varphi \quad (1)$$

Then, using Eq. 1 in the continuity equation, $\nabla \cdot \mathbf{v} = 0$, one obtains that φ satisfies the Laplace equation, $\nabla^2\varphi = 0$.

The boundary condition on the rotor blade is

$$\mathbf{v} \cdot \mathbf{n} = \mathbf{v}_b \cdot \mathbf{n} \quad \text{or} \quad \frac{\partial\varphi}{\partial n} = \mathbf{v}_b \cdot \mathbf{n} \quad (2)$$

The frame of reference is assumed to be connected with the undisturbed air; thus the condition at infinity is $\mathbf{v} = 0$ or $\varphi = 0$. Indicating with $\Delta\varphi = \varphi_u - \varphi_l$ (with u =upper, l =lower) the potential discontinuity across the wake, and using Bernoulli's theorem with the boundary condition on the wake $\Delta p = 0$ one obtains (see Refs. 8 or 11 for details)

$$\frac{D_w}{Dt}(\Delta\varphi_w) = 0 \quad (3)$$

with $\frac{D_w}{Dt} = \frac{\partial}{\partial t} + \mathbf{v}_w \cdot \nabla$, where $\mathbf{v}_w = \frac{1}{2}(\nabla\varphi_u + \nabla\varphi_l)$ is the velocity of a wake-point \mathbf{x}_w . The above equation may be integrated to yield

$$\Delta\varphi = \text{constant in time following a wake point} \quad (4)$$

In addition, the condition that concentrated vortices do not exist at the trailing edge, yields the result

$$\Delta\varphi(\mathbf{x}_w^{TE}, t) = \varphi(\mathbf{x}_u^{TE}, t) - \varphi(\mathbf{x}_l^{TE}, t) \quad (5)$$

where \mathbf{x}_w^{TE} is a wake point at the trailing edge whereas \mathbf{x}_u^{TE} and \mathbf{x}_l^{TE} are points of the upper and lower sides of the blade, also at the trailing edge (see Refs. 11 and 14 for a detailed analysis of this point).

The above equations may be used to obtain the solution for φ . Once φ is known, the velocity may be evaluated using Eq. 1. Then the pressure may be evaluated using Bernoulli's theorem

$$\frac{\partial\varphi}{\partial t} + \frac{1}{2}|\mathbf{v}|^2 + \frac{p}{\rho} = \frac{p_\infty}{\rho} \quad (6)$$

In order to solve this problem it is convenient to recast it as an integral equation. The integral equation used by Morino et al.⁸ is a particular case of that developed by Morino^{15,16}; using the classical Green's function method, for the general case of potential compressible flows for bodies having arbitrary shapes and motions. For the problem of interest here - incompressible flows - starting from the Green theorem applied to a surface σ surrounding both body and wake, and then collapsing the portion of σ surrounding the wake into a single surface, σ_w , one obtains (see Ref. 8 for details)

$$E(\mathbf{x})\varphi(\mathbf{x}) = \iint_{\sigma_b} \left[\frac{\partial\varphi}{\partial n} \left(\frac{-1}{4\pi|\mathbf{x}-\mathbf{y}|} \right) - \varphi \frac{\partial}{\partial n} \left(\frac{-1}{4\pi|\mathbf{x}-\mathbf{y}|} \right) \right] d\sigma(\mathbf{y}) - \iint_{\sigma_w} \Delta\varphi \frac{\partial}{\partial n} \left(\frac{-1}{4\pi|\mathbf{x}-\mathbf{y}|} \right) d\sigma(\mathbf{y}) \quad (7)$$

where σ_b is the (closed) surface of the rotor blade and σ_w is the (open) surface of the wake of the rotor blade (\mathbf{n} on σ_w is the normal on the upper side). Furthermore

$$\begin{aligned} E(\mathbf{x}) &= 1 - \Omega(\mathbf{x})/4\pi = 1 && \text{for } \mathbf{x} \text{ outside } \sigma_b \\ &= \frac{1}{2} && \text{for } \mathbf{x} \text{ on } \sigma_b \text{ (regular point)} \\ &= 0 && \text{for } \mathbf{x} \text{ inside } \sigma_b \end{aligned} \quad (8)$$

If \mathbf{x} is on σ_b , Eq. 7 is an integral equation relating the potential ϕ to its normal derivative, $\partial\phi/\partial n$ (known from the boundary condition Eq. 2), and its discontinuity across the wake, $\Delta\phi$ (evaluated using Eqs. 4 and 5). The velocity of the points of the wake is given by Eq. 3, and is evaluated by taking the gradient of Eq. 7. The evolution of the wake geometry is obtained from the velocity of the wake points.

Note that in the above formulation, the wake of the rotor is represented as a layer of doublets and therefore, in the following, it will be referred to as the doublet-wake formulation.

3. Potential Vortex-Wake Formulation

An alternate formulation for potential flows, fully equivalent to that summarized above, was proposed in Ref. 11, and is presented here. This formulation has the advantage of being easily extended to viscous flows (see Section 4). The velocity is expressed as

$$\mathbf{v} = \nabla(\phi + \phi_w) = \nabla\phi + \mathbf{w} \quad (9)$$

where ϕ is continuous across the wake, whereas

$$\mathbf{w}(\mathbf{x}) = \nabla\phi_w = \nabla \iint_{\sigma_w} \Delta\phi_w \frac{\partial}{\partial n} \left(\frac{1}{4\pi|\mathbf{x}-\mathbf{y}|} \right) d\sigma(\mathbf{y}) \quad (10)$$

is the contribution to the velocity due to the potential discontinuity across the wake.

Using the continuity equation, one obtains that the potential ϕ satisfies the Laplace equation in the whole flow field (including the wake points, since, by definition, ϕ is continuous across the wake). Therefore it also satisfies the integral relation

$$E(\mathbf{x})\phi(\mathbf{x}) = - \iint_{\sigma_b} \left[\frac{\partial\phi}{\partial n} \left(\frac{1}{4\pi|\mathbf{x}-\mathbf{y}|} \right) - \phi \frac{\partial}{\partial n} \left(\frac{1}{4\pi|\mathbf{x}-\mathbf{y}|} \right) \right] d\sigma(\mathbf{y}) \quad (11)$$

The boundary condition for ϕ on the surface of the body is (see Eqs. 2 and 9)

$$\frac{\partial\phi}{\partial n} = \mathbf{v}_b \cdot \mathbf{n} - \mathbf{w} \cdot \mathbf{n} \quad \text{on } \sigma_b \quad (12)$$

Using Bernoulli's theorem and recalling that $\Delta\phi = 0$, one obtains $\frac{D\phi}{Dt}(\Delta\phi_w) = 0$ or (see Eq. 4)

$$\Delta\phi_w = \text{constant in time following a wake point} \quad (13)$$

(Eq. 13 is fully equivalent to Eq. 4).

The trailing-edge condition is now

$$\Delta\phi_w(\mathbf{x}_w^{TE}, t) = \phi(\mathbf{x}_u^{TE}, t) - \phi(\mathbf{x}_l^{TE}, t) \quad (14)$$

where \mathbf{x}_w^{TE} is a wake point at the trailing edge whereas \mathbf{x}_u^{TE} and \mathbf{x}_l^{TE} are points of the upper and lower sides of the blade, also at the trailing edge (see Ref. 11 for a detailed analysis of this point).

As mentioned above, the alternate formulation presented above is fully equivalent of that of Ref. 8 (the equivalence of the two formulations is demonstrated in Appendix A). However it has a major advantage that is not immediately obvious. Because of the well known equivalence between doublet layers and vortex layers (see, e.g., Refs. 17-19),

$$\begin{aligned} \nabla \iint_{\sigma} D(\mathbf{y}) \frac{\partial}{\partial n} \left(\frac{1}{4\pi|\mathbf{x}-\mathbf{y}|} \right) d\sigma(\mathbf{y}) = \\ \nabla \times \left(\iint_{\sigma} \gamma(\mathbf{y}) \frac{1}{4\pi|\mathbf{x}-\mathbf{y}|} d\sigma(\mathbf{y}) + \oint_C D(\mathbf{y}) \frac{1}{4\pi|\mathbf{x}-\mathbf{y}|} d\mathbf{y} \right) \end{aligned} \quad (15)$$

with $\boldsymbol{\gamma} = \mathbf{n} \times \nabla_t D$ (where ∇_t is the surface gradient), Eq. 10 may be rewritten as

$$\mathbf{w}(\mathbf{x}) = \nabla \times \left(\iint_{\sigma_w} \boldsymbol{\gamma}(\mathbf{y}) \frac{1}{4\pi|\mathbf{x} - \mathbf{y}|} d\sigma(\mathbf{y}) + \int_{TE} \Delta\phi_w(\mathbf{y}) \frac{1}{4\pi|\mathbf{x} - \mathbf{y}|} d\mathbf{y} \right) \quad (16)$$

with

$$\boldsymbol{\gamma} = \mathbf{n} \times \nabla_t(\Delta\phi_w) \quad (17)$$

where ∇_t is the tangential gradient. The expression for \mathbf{w} in Eq. 16 is the well known Biot-Savart law for the velocity induced by a vortex layer (the effect of the presence of the wake is introduced as a contribution to the boundary conditions on $\partial\phi/\partial n$ (see Eq. 12) through the velocity induced by the vortex layer, as in the Prandtl lifting-line theory). Therefore this formulation will be referred to as the vortex-wake formulation in order to emphasize that it is convenient to interpret the wake as a vortex layer (even though the doublet-layer interpretation is also legitimate); the advantage of this interpretation is discussed in Section 4.

Note that in order to complete the vortex-layer formulation one needs an equation for the transport of $\boldsymbol{\gamma}$. This is derived in Appendix B.

4. Viscous Formulation

The advantage of the expression for \mathbf{w} given in Eq. 16 is that this expression may be derived without using the assumption of potential flows: the formulation may be obtained directly from the Helmholtz decomposition (scalar/vector potential formulation; see Ref. 11 for details). More specifically, if the vortex layer has a non-zero thickness, the flow cannot be represented in terms of a velocity potential. Therefore the first expression for \mathbf{w} (Eq. 10) is completely meaningless in this case. However, the alternate form given in Eq. 16 may be considered as a computational approximation of the correct expression

$$\mathbf{w}(\mathbf{x}) = \nabla \times \iiint_{V_w} \frac{\boldsymbol{\omega}(\mathbf{y})}{4\pi|\mathbf{x} - \mathbf{y}|} dV(\mathbf{y}) \quad (18)$$

where $\boldsymbol{\omega} = \nabla \times \mathbf{v}$ is the vorticity. The solution of the transport equation for the vorticity is required in order to obtain $\boldsymbol{\omega}$. This is accomplished by using the formulation of Ref. 20, which gives the solution of the problem in terms of material contravariant components of $\boldsymbol{\omega}$ (the actual approach used is outlined in Appendix B).

As mentioned above, Eq. 18 may be derived directly from first principles, using the Helmholtz decomposition theorem. The essence of the approach used here may be summarized as follows: in the potential-flow formulation of Ref 8, the wake is treated as a doublet layer, and hence, is restricted to zero thickness. On the other hand, in the potential-flow formulation presented in Section 3, the wake may be conceived of either as a doublet layer or, more conveniently, as a vortex layer. The advantage of the vortex-layer interpretation is that (unlike doublet layers) vortex layers are not meaningless for non-zero thickness. This implies that the wake thickness does not have to be equal to zero, and therefore, the formulation can be used to introduce (in a *gradual* fashion!) the effects of viscosity and eddy-viscosity.

Finally, a brief discussion about the legitimacy (and rigor) of Eq. 18: a rigorous proof that Eq. 18 is correctly describing the effect of the vorticity in the wake region is given in Refs. 11 and 14. In addition, Ref. 14 shows that the effect of the vorticity in the boundary layer region may be included in the formulation by introducing the concept of 'defect velocity', i.e., the difference between the actual solution (which includes the effects of the vorticity in the boundary layer) and the harmonic continuation (the three-dimensional equivalent of the analytic continuation) of the external velocity. The only change required to include the vorticity in the boundary layer region is to modify Eq. 12 to read $\partial\phi/\partial n = \mathbf{v}_b \cdot \mathbf{n} - \mathbf{w} \cdot \mathbf{n} - \mathbf{v}_d \cdot \mathbf{n}$ on σ_b where \mathbf{v}_d is the 'defect velocity'. By definition, \mathbf{v}_d is solenoidal (i.e., divergence free) and is equal to zero outside the boundary layer region. This

allows one to obtain an expression for $-\mathbf{v}_d \cdot \mathbf{n}$ which is nearly identical to the transpiration velocity introduced by Lighthill²¹. As shown by Morino¹⁴ the above formulation (unlike to Lighthill's) is exact, in the sense that it is fully equivalent to the original Navier-Stokes equations.

5. Computational Algorithm

For the purpose of numerical computations, the rotor blade surface is divided into quadrilateral elements with boundaries in the chordwise and radial directions. Typically three elements chordwise and seven elements spanwise (for upper and lower surfaces) were used for a total of 42 elements per blade.

The wake originating at the trailing edge of the blade and spiraling downstream for increasing azimuth angle is similarly discretized into quadrilateral elements. Typically, five wake spirals were included in the computations with each wake spiral being divided into twelve elements in the azimuth direction (i.e., one element for every 30 degrees), and seven elements in the radial direction for a total of 84 elements representing one entire wake spiral. In the near wake (first one or two spirals), the velocity at each wake node is evaluated at each time step. In the intermediate wake (last three or four spirals), the velocity is prescribed; for the results presented here, the velocity prescribed for the intermediate spirals is the one that would generate a Landgrebe²⁴ wake. A far wake model (a source disk) of the type used by Summa⁶ is also employed.

The integral equation (Eq. 7 for the doublet-wake formulation, or Eq. 11 for the vortex-wake formulation) was discretized accordingly with collocation points at the centers of the blade elements. This yields a set of algebraic equations with the unknowns being the values at the collocation points of φ for the doublet-wake formulation, or ϕ for the vortex-wake formulation (see Bharadvaj and Morino¹⁵ for details).

In order to avoid the well-known problems of the start-up vortex (see, e.g., Summa²), the initial vorticity distribution on the wake was assumed to be that corresponding to the steady-state solution as obtained with a prescribed wake geometry. A classical wake (modified to have a radial contraction) with a pitch $\Delta z = 2\pi R\sqrt{C_T/2}$ (and C_T prescribed) was used for the initial wake geometry. The tip vortex location was moved upward by one-fourth of the pitch (this modification was introduced to improve the rate of convergence of the wake geometry).

The effects of viscosity are included in the analysis by allowing the vorticity to diffuse, i.e., by representing the wake by vortex filaments having a finite core. The size of the vortex core is varied in time according an expression obtained from the vorticity transport equation; the thickness of the wake at the trailing edge and the eddy viscosity coefficient are prescribed (see Morino and Bharadvaj¹¹ for details).

For other less important issues (such as the motion of the root vortex) the reader is referred to Ref. 11.

6. Numerical Results

Only a sample of results for a rotor in hover are presented here to show the capability of the method. An extensive collection of results exploring various parameters, have been obtained with this formulation and are presented in detail by Morino and Bharadvaj¹¹. Unless stated otherwise, only the first wake spiral was treated as being free while the other four were treated as the intermediate wake (i.e., with prescribed velocity). The intensity of the sink disk was prescribed based on the mass flux, which was obtained from a combination of theoretical (actuator disk) and experimental (Landgrebe²⁴) considerations. Figures 1 to 3 are for a single bladed rotor with radius of 17.5 ft, root cut-out of 2.33 ft, constant chord of 1.083 ft, collective pitch of 10.61°, washout angle of 5.0° and blade rotational speed of 355.0 rpm.

The development of the wake with time is presented in Figures 1.A through 1.F; the time interval between successive figures is six time steps which corresponds to a half-revolution of the rotor blade; the figures show the radial cross-sections of the wake for a

single bladed rotor. (Note that all the sections shown in the figures are physically located in different planes; the cross-sections are all plotted on the same plane to show the evolution of the wake in a compact form. Four cross-sections per wake spiral, 90° apart from each other, are shown; this is specifically indicated in Figure 1.A). It can be seen that the initial frozen wake that was assumed in Figure 1.A undergoes rapid change as the rotor begins to move. Specifically, the region near the rotor tip tends to roll up into the tip vortex, whereas the inboard vortex sheet has a strong downward movement. Also it may be noted that the solution is always smooth, an indication of the robustness of the algorithm.

Figure 2 shows two different load distributions for the single-bladed rotor of Figure 1. One was obtained by allowing only one wake spiral to be free (with prescribed velocity for the remaining four spirals). The second loading was obtained with the first two wake spirals being free in the analysis. As can be seen, the load distributions are very similar indicating that reasonable results can be obtained by allowing only one wake spiral to be free.

Figure 3 shows the variation in the load distribution with time for the problem of Figure 1. It can be seen that the loading changes as the wake geometry varies, however the change is not very dramatic. Figure 3 also shows a comparison between the present results with the computational (generalized wake) results of Rao and Schatzle²⁵. Note that the thrust coefficient C_T predicted by the present method is 0.00158 compared to 0.00186 used by Rao and Schatzle in their generalized wake analysis.

New results, obtained since the publication of Ref. 11 are presented here in Figures 4 and 5. Figure 4, for a two-bladed rotor using the same blade as the rotor of Figure 1, shows a comparison of the wake geometry obtained from the present analysis with the generalized wake of Landgrebe²⁴. The agreement in the locations of the inboard vortex sheet is quite good. The region of strong vorticity roll-up predicted by the present results is located very close to the tip-vortex location of Landgrebe²⁴.

The last figure is for a different single bladed rotor: radius of 24.0 inches, root cut-out of 6.0 inches and a constant chord of 5.0 inches. This rotor was tested at a collective pitch setting of 6.2° (no twist) and rotational speed of 1000 rpm. Figure 5 shows that the radial location of the tip vortex, for the first wake spiral, predicted by the present formulation compare well with the experimental results of Shivananda²⁶.

7. Conclusions

A new unified integral-equation approach for the potential and viscous free-wake analysis of helicopter rotors has been presented. It may be worth pointing out that the viscous-flow formulation is very similar to the potential-flow formulation of Ref. 8 (see Section 2), if 'artificial viscosity' is used in the evaluation of the velocity of the wake points. Actually, as shown in Ref. 11, this yields results that are practically indistinguishable from those obtained from the use of actual eddy-viscosity in the vortex-layer formulation. However, there is a big conceptual difference between the two cases. In the potential-flow formulation, 'artificial viscosity' is just what its name implies: an artificial way to enhance the numerical stability by increasing the vortex size in the evaluation of the velocity of the wake points. This introduces an inconsistency in the treatment of the wake since it is regarded as having zero-thickness in the integral equation, whereas the velocity is computed as the gradient of a vortex layer with finite-thickness (stemming from the artificial-viscosity approximation). The formulation of Section 4, on the other hand, is fully consistent: the same wake description (finite-thickness or zero-thickness) is used both in the integral equation and in the expression for the velocity.

Results obtained indicate that, for appropriate values of empirical parameters (e.g., thickness of the wake at the trailing edge, eddy-Reynolds number, intensity of the far wake sink disk), the solution reaches steady-state, with the wake converging to a smooth geometry and the sectional lift distribution in good agreement with the numerical results of Rao and Schatzle²⁵ and with the experimental ones of Landgrebe²⁴ and Shivananda²⁶. Most of the computations were performed on a VAX-780 computer. The vortex-wake

formulation requires approximately the same amount of computer time as the doublet-wake formulation.

In summary, we may conclude that the new formulation presented here has much broader applicability than the formulation for potential flows (it also appears to be more robust), while requiring approximately the same amount of computation time.

In terms of further development of the method, we believe that the most important item to be addressed is the higher-order formulation for the wake. A second item which requires further improvement is the modelling for the intermediate and far wakes: the parameters describing the models (now given as input data) should be self-adjusting. Additional work is also needed in connection with the turbulence modelling and the boundary layer analysis. Work on these issues is currently under way.

Acknowledgements: This work was partially supported by Contract DAAG29-83-K-0050 from the U.S. Army Research Office to Boston University.

REFERENCES

1. Scully, M.B., 'Computation of Helicopter Rotor Wake Geometry and its Influence on Rotor Harmonic Airloads,' MIT ASRL-TR-176-1, March 1971.
2. Summa, J.M., 'Potential Flow about Impulsively Started Rotors,' *Journal of Aircraft*, Vol. 13, No. 4, April 1976, pp. 317-319.
3. Suci, E.O., Morino, L., 'Nonlinear Steady Incompressible Lifting-Surface Analysis with Wake Roll-Up,' *AIAA Journal*, Vol. 15, No. 1, January 1977, pp. 54-58.
4. Summa, J.M., and Clark, D.R., 'A Lifting-Surface Method for Hover/Climb Airloads,' 35th Annual Forum of American Helicopter Society, Washington, D.C., May 1979.
5. Pouradier J.M., and Horowitz, E., 'Aerodynamic Study of a Hovering Rotor,' Sixth European Rotorcraft and Powered Lift Aircraft Forum, Paper No. 26, Bristol, England, September 1980.
6. Summa, J.M., 'Advanced Rotor Analysis Method for the Aerodynamics of Vortex/Blade Interactions in Hover,' Eighth European Rotorcraft and Powered Lift Aircraft Forum, Paper No. 2.8, Aix-en-Provence, France, August 31-September 3, 1982.
7. Miller, R.H., 'Application of Fast Free Wake Analysis Techniques to Rotors,' Eighth European Rotorcraft and Powered Lift Aircraft Forum, Aix-en-Provence, France, August 31-September 3, 1982.
8. Morino, L., Kaprielian, Z., Jr., and Sipcic, S.R. 'Free Wake Analysis of Helicopter Rotors,' *Vertica*, Vol. 9, No. 2, 1985, pp. 127-140.
9. Sipcic, S.R., and Morino, L., 'Wake Dynamics for Incompressible and Compressible Flows,' in *Computational Methods in Potential Aerodynamics* (Ed.: L. Morino), Springer Verlag, 1985.
10. Kandil, O.A., 'Wake Dynamics in Incompressible Flows,' *Computational Methods in Potential Aerodynamics* (Ed.: L. Morino), Springer Verlag, 1985.
11. Morino, L., and Bharadvaj, B.K., 'Two Methods for Viscous and Inviscid Free-Wake Analysis of Helicopter Rotors,' CCAD-TR-85-04-R, Boston University, 1985.
12. Morino, L., Bharadvaj, B.K., and Del Marco, S.P., 'Helmholtz Decomposition and Navier-Stokes Equations', *Computational Mechanics '86*, Vol. 2, Springer Verlag, 1986, pp. VII-181-186
13. Bharadvaj, B. K., and Morino, L., 'Free-Wake Analysis of Helicopter Rotors: A Boundary Element Approach', BETECH 86, Proceedings of the 2nd Boundary Element Technology Conference, MIT, USA, pp. 291-303, Computational Mechanics Publications, 1986.
14. Morino, L. 'Helmholtz Decomposition Revisited: Vorticity Generation and Trailing Edge Condition. Part I - Incompressible Flows', *Computational Mechanics*, Vol. 1, No. 1, 1986, pp. 65-90.
15. Morino, L., 'Unsteady Compressible Flow Around Lifting Bodies: General Theory,' AIAA 11th Aerospace Sciences Meeting, Washington, D.C., AIAA Paper No. 73-196,

January 1973.

16. Morino, L., 'A General Theory of Unsteady Compressible Potential Aerodynamics,' NASA CR-2464, December 1974.

17. Batchelor, G.K., *An Introduction to Fluid Dynamics*, Cambridge University Press, 1967.

18. Campbell, R.G., *Foundations of Fluid Flow Theory*, Addison-Wesley Publishing Co., Reading, Mass., 1973, p. 258

19. Soohoo, P., Noll, R.B., Morino, L., and Hamm, N.D., (1978), 'Rotor Wake Effects on Hub/Pylon Flow,' Vol. I, Theoretical Formulation, Applied Technology Laboratory, U.S. Army Research and Technology Laboratories (AVRADCOM), Fort Eustis, Va., USARTL-TR-78-1A, p. 108.

20. Morino, L. 'Material Contravariant Components, Vorticity Transport and Vortex Theorems', AIAA J. Vol. 24, No. 3, 1986, pp. 256-258.

21. Lighthill, M.J., 'On Displacement Thickness,' Journal of Fluid Mechanics, Vol. 4, 1958, pp. 383-392.

22. Lamb, H., *Hydrodynamics*, 6th ed., Cambridge University Press, 1932.

23. Sokolnikoff, I. S., *Tensors Analysis* Wiley, N. Y., 1951.

24. Landgrebe, A.J., 'An Analytical Method for Predicting Rotor Wake Geometry', Journal of the American Helicopter Society, Vol. 14, No. 4, 1969, pp. 20-32.

25. Rao, B.M. and Schatzle, P.R., 'Analysis of Unsteady Airloads of Helicopter Rotors in Hover', AIAA Paper 77-159, AIAA 15th Aerospace Sciences Meeting, Los Angeles, USA, 1977.

26. Shivananda, T.P., 'Pressure Measurements Near the Tip of a Hovering Model Rotor Blade and a Preliminary Investigation of the Flow in the Rotor Wake', Ph.D. Thesis, School of Aerospace Engineering, Georgia Institute of Technology, Atlanta, USA, 1977.

Appendix A. Equivalence of Doublet- and Vortex-Wake Formulations

Presented in this Appendix is the equivalence between the doublet wake formulation of Morino et al.⁸, and the vortex-wake formulation of Morino and Bharadvaj¹¹.

In order to facilitate the discussion, consider Eq. 7 and note that, following Lamb²² this equation may be generalized by allowing a "fictitious" incompressible potential flow inside σ_b : this interior flow has a velocity $\mathbf{v}_I = \nabla\varphi_I$, where φ_I has an integral representation of the type

$$E_I(\mathbf{x})\varphi_I(\mathbf{x}) = \iint_{\sigma_b} \left[\frac{\partial\varphi_I}{\partial n_I} \frac{-1}{4\pi|\mathbf{x}-\mathbf{y}|} - \varphi_I \frac{\partial}{\partial n_I} \left(\frac{-1}{4\pi|\mathbf{x}-\mathbf{y}|} \right) \right] d\sigma(\mathbf{y}) \quad (A.1)$$

This equation is obtained by following the same procedure used to obtain Eq. 7, but using the volume inside σ_b instead of that outside; therefore $E_I = 1 - E$ and $\mathbf{n}_I = -\mathbf{n}$. Combining Eqs. 7 and A.1 one obtains (using the above expressions)

$$\begin{aligned} E(\mathbf{x})\varphi(\mathbf{x}) + (1 - E(\mathbf{x}))\varphi_I(\mathbf{x}) = & - \iint_{\sigma_b} \left[\frac{\partial}{\partial n} (\varphi - \varphi_I) \frac{1}{4\pi|\mathbf{x}-\mathbf{y}|} - (\varphi - \varphi_I) \frac{\partial}{\partial n} \left(\frac{1}{4\pi|\mathbf{x}-\mathbf{y}|} \right) \right] d\sigma(\mathbf{y}) \\ & + \iint_{\sigma_w} \Delta\varphi \frac{\partial}{\partial n} \left(\frac{1}{4\pi|\mathbf{x}-\mathbf{y}|} \right) d\sigma(\mathbf{y}) \end{aligned} \quad (A.2)$$

which is the generalized integral equation for potential flows. Note that φ_I satisfies Eq. A.1 and is otherwise completely arbitrary (since $E_I \equiv 0$ outside σ_b).

On the other hand, Eqs. 10 and 11 may be combined to yield

$$\begin{aligned} E(\mathbf{x})\phi(\mathbf{x}) + \phi_w(\mathbf{x}) = & - \iint_{\sigma_b} \left[\frac{\partial\phi}{\partial n} \frac{1}{4\pi|\mathbf{x}-\mathbf{y}|} - \phi \frac{\partial}{\partial n} \left(\frac{1}{4\pi|\mathbf{x}-\mathbf{y}|} \right) \right] d\sigma(\mathbf{y}) \\ & + \iint_{\sigma_w} \Delta\phi_w \frac{\partial}{\partial n} \left(\frac{1}{4\pi|\mathbf{x}-\mathbf{y}|} \right) d\sigma(\mathbf{y}) \end{aligned} \quad (A.3)$$

Note that (see Eqs. 1 and 9) the velocity is given by $\mathbf{v} = \nabla\varphi = \nabla(\phi + \phi_w)$ with (see Eqs. 2, 9 and 11)

$$\frac{\partial\varphi}{\partial n} = \frac{\partial\phi}{\partial n} - \frac{\partial\phi_w}{\partial n} = \mathbf{v}_b \cdot \mathbf{n} \quad (A.4)$$

Therefore, one expects that, at least outside σ_b , $\varphi = \phi + \phi_w$. Substituting this equation into Eq. A.3, one obtains (note that $\Delta\phi = 0$ on the wake)

$$\begin{aligned} E(\mathbf{x})\varphi(\mathbf{x}) + (1 - E(\mathbf{x}))\phi_w(\mathbf{x}) = & - \iint_{\sigma_b} \left[\frac{\partial}{\partial n}(\varphi - \phi_w) \frac{1}{4\pi|\mathbf{x} - \mathbf{y}|} - (\varphi - \phi_w) \frac{\partial}{\partial n} \left(\frac{1}{4\pi|\mathbf{x} - \mathbf{y}|} \right) \right] d\sigma(\mathbf{y}) \\ & + \iint_{\sigma_w} \Delta\varphi \frac{\partial}{\partial n} \left(\frac{1}{4\pi|\mathbf{x} - \mathbf{y}|} \right) d\sigma(\mathbf{y}) \end{aligned} \quad (A.5)$$

By comparing Eqs. A.2 and A.5 we may conclude that the vortex-wake formulation coincides with the doublet-wake formulation as this is extended by adding a 'fictitious' internal flow $\varphi_I = \phi_w$.

Appendix B. On Vorticity Transport for Vortex Layers

In this Appendix the equation for the transport of the surface distribution of vorticity γ , is derived. The extension of the equation to wakes having small but finite thickness are also discussed, for both inviscid and viscous flows. Details of the formulation are given in Ref. 11.

Recall that if ξ^α are curvilinear coordinates on a surface σ , then the tangential gradient is given by (see, e.g., Ref. 23)

$$\nabla_t f = \mathbf{a}^1 \frac{\partial f}{\partial \xi^1} + \mathbf{a}^2 \frac{\partial f}{\partial \xi^2} \quad (B.1)$$

where \mathbf{a}^α are the contravariant base vectors on σ which are such that

$$\mathbf{a}^1 \times \mathbf{n} = - \frac{\mathbf{a}_2}{|\mathbf{a}_1 \times \mathbf{a}_2|} \quad \text{and} \quad \mathbf{a}^2 \times \mathbf{n} = \frac{\mathbf{a}_1}{|\mathbf{a}_1 \times \mathbf{a}_2|} \quad (B.2)$$

Using Eqs. 17, B.1 and B.2, one obtains

$$\boldsymbol{\gamma} = \mathbf{n} \times \nabla_t(\Delta\phi_w) = \gamma^1 \mathbf{a}_1 + \gamma^2 \mathbf{a}_2 \quad (B.3)$$

where

$$\gamma^1 = \frac{-1}{|\mathbf{a}_1 \times \mathbf{a}_2|} \frac{\partial(\Delta\phi_w)}{\partial \xi^2} \quad \text{and} \quad \gamma^2 = \frac{1}{|\mathbf{a}_1 \times \mathbf{a}_2|} \frac{\partial(\Delta\phi_w)}{\partial \xi^1} \quad (B.4)$$

are the contravariant components of $\boldsymbol{\gamma}$ (Ref. 23).

Next assume that ξ^α is a system a material coordinates (i.e., a system of coordinates that moves with the material points). Since $\Delta\phi_w$ is constant in time following a wake point (i.e., keeping ξ^1 and ξ^2 constant) one obtains that $\gamma^\alpha |\mathbf{a}_1 \times \mathbf{a}_2|$ is constant in time following a wake point or $\frac{D}{Dt}(\gamma^\alpha |\mathbf{a}_1 \times \mathbf{a}_2|) = 0$ which is the desired transport equation for the vorticity of a zero-thickness vortex layer.

This is related to the result by Morino²⁰ that, for an incompressible inviscid fluid, the substantial derivative of the material contravariant components of $\boldsymbol{\omega}$ are equal to zero. As shown in detail in Ref. 11, Eq. B.6 is valid for thin wakes (for both inviscid and viscous flows): in this case $\boldsymbol{\gamma}$ is the integral of $\boldsymbol{\omega}$ over the thickness of the wake (this result is obtained by integrating, over the wake thickness, the result of Ref. 20 given above).

Also in Ref. 11 it is shown that, for inviscid incompressible flows, the product of a material surface element times the wake thickness is constant in time. A differential equation for the evolution of the wake thickness for viscous incompressible fluids is also derived in Ref. 11.

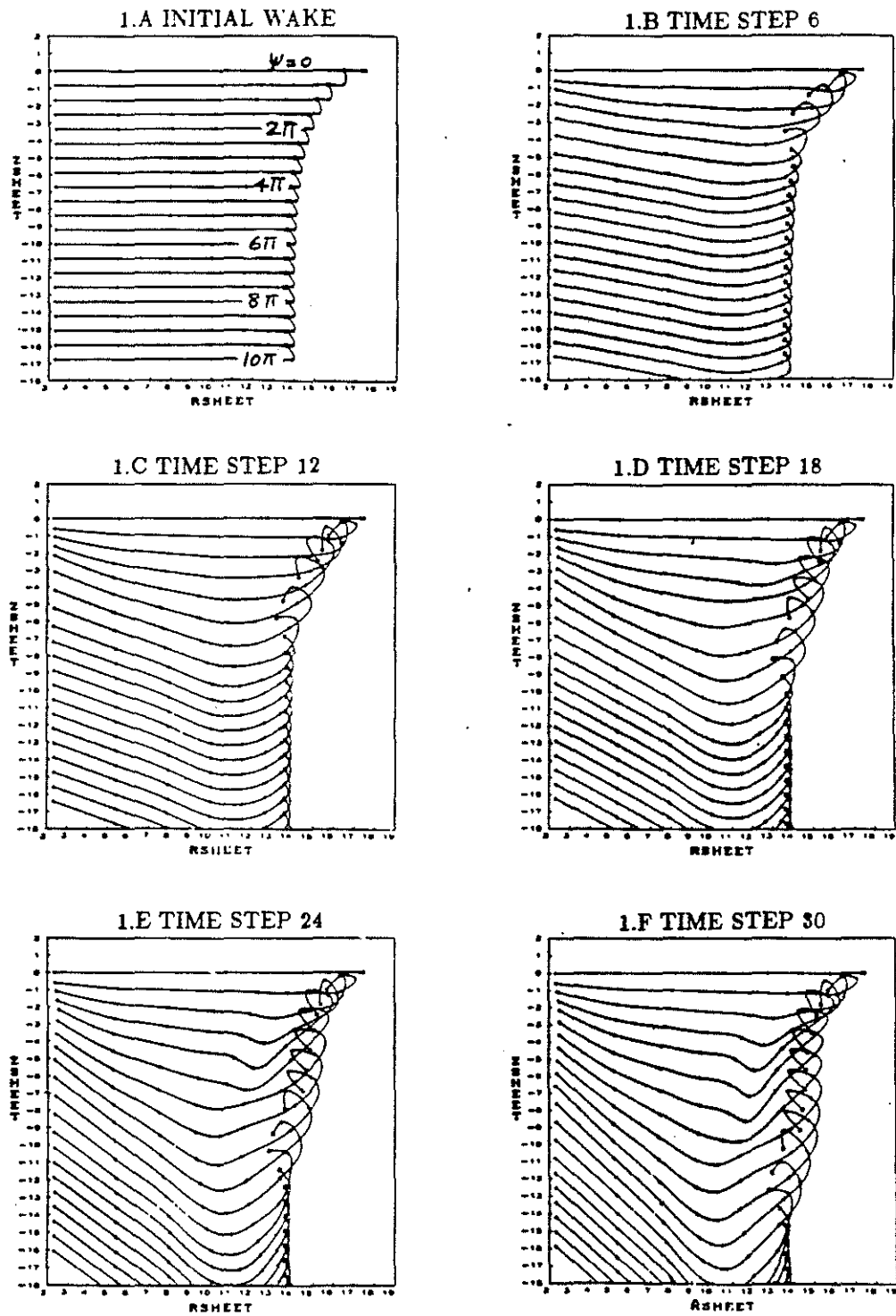


Figure 1. Development of the wake with time

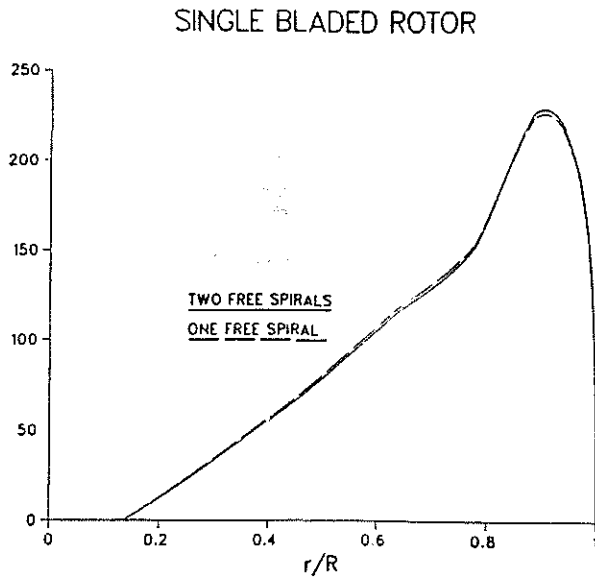


Figure 2. One vs Two Free Spirals

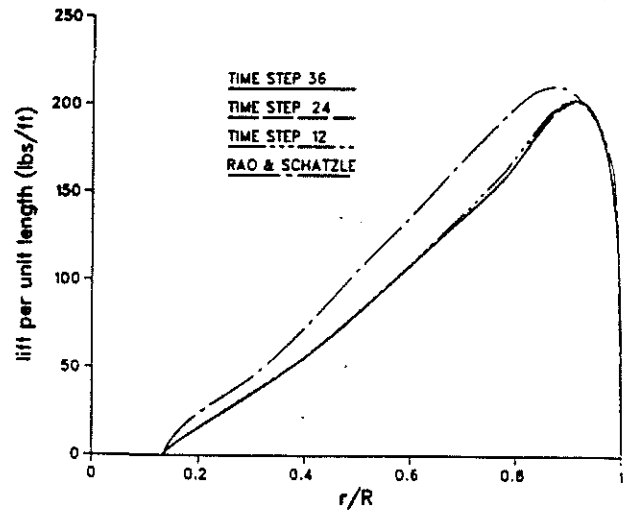


Figure 3. Development of blade loading

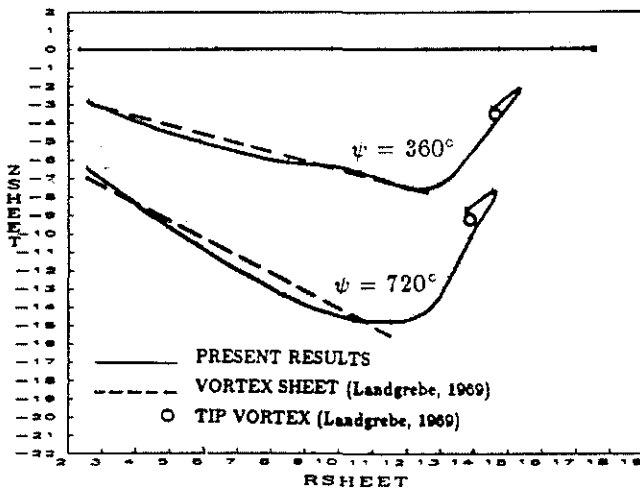


Figure 4. Comparison of wake geometry with experiments of Ref. 24

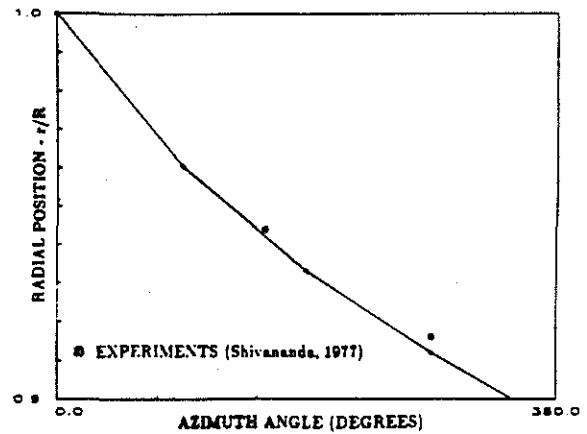


Figure 5. Comparison of tip vortex location with experiments of Ref. 26